Polym. Bull. (2011) 66:721–734
DOI 10.1007/s00289-010-0301-2

ORIGINAL PAPER

Superabsorbent nanocomposite hydrogels based on intercalation of chitosan into activated bentonite

Hazem El-Sherif · Mansour El-Masry

Received: 17 January 2010 / Revised: 6 May 2010 / Accepted: 16 May 2010 /
Published online: 22 May 2010

Abstract Superabsorbent polymers, composed of acrylamide (Am) and 2-acrylamido-2-methyl-1-propane sulfonic acid, were prepared by the solution crosslinking polymerization technique. The effect of the ionic monomer content was correlated with the equilibrium swelling capacity. The swelling capacity was augmented up to 94 g/g by increasing the concentration of the ionic monomer. Intercalation of bentonite clay, by chitosan solution, was performed by two techniques, namely, microwave irradiation and heating. The basal spacing of bentonite increased from 1.21 to 1.31 nm for the former and to 1.4 nm for the latter. Specific interaction of bentonite with –OH group of chitosan through hydrogen bonding was estimated by FT-IR. Also, TEM showed a layered morphology due to the penetration of chitosan chains into bentonite silicate layers. Different amount of the intercalated clay was dispersed in the aforementioned monomers aiming at preparing superabsorbent composites. The clay showed an exfoliated structure in the polymer matrix while the composite was porous, with a three-dimensional interconnected microstructure as proved by SEM. The prepared composites had a higher absorption capacity up to 180 g/g and a better thermal stability than the corresponding hydrogel.

Keywords Superabsorbent · Hydrogels · Intercalation · Exfoliation · Nanocomposite

Introduction

Superabsorbents are a loosely crosslinked network of hydrophilic polymers that can absorb and retain a lot of aqueous fluids, and the absorbed water is hardly removable

H. El-Sherif (✉) · M. El-Masry
Polymers & Pigments Department, National Research Center, El-Bohouth Street, Dokki, Cairo, Egypt
e-mail: elsherifhazem@hotmail.com

even under some pressure. The ability of polymer gels to undergo a substantial swelling and a collapsing, up to 1,000 times in volume, as a function of their environment is one of the most notable properties of these materials. Their affinity for water makes them useful, especially for agriculture, personal hygiene products, industrial absorbents, medicine, and cosmetics. The most efficient water absorbents are polymer networks that carry dissociated ionic functional groups [1–6].

In 1985, an inorganic–organic composite (Superabsorbent Polymer Clay composite, SAPC) was prepared by intercalating acrylamide (Am) into an expandable smectitic clay, e.g., bentonite (BENT) using γ-ray radiation-induced polymerization. The new material showed a high water absorption capacity [7].

Recently, the development and the characterization of nanostructured polymer–clay composites have received special attention due to their advantages compared with that of traditional polymer composites. Minimal additions of nanoclays enhance the nanocomposites performance properties significantly because of the large contact area between a polymer and a clay on a nanoscale [4].

The important characteristics pertinent to the application of clay minerals in polymer nanocomposites are their richest intercalation chemistry, high strength and stiffness, high aspect ratio of individual platelets, abundance in nature and low cost. First, their unique layered structure and high intercalation capabilities allow them to be chemically modified and compatible with polymers, which make them particularly attractive in the development of clay-based polymer nanocomposites. In addition, their relatively low layer charge ($x = 0.2$–0.6) means a relatively weak force between adjacent layers, making the interlayer cations exchangeable [8]. Monomers and polymers can enter the interlayer distance of a modified clay in the process of polymer nanocomposites preparation [9].

With the addition of small amounts of intercalated nanofillers into different polymer matrix (e.g., conjugated, thermoplastic, and thermosetting polymers), the as-prepared composites exhibit substantial increase in various physical and chemical properties, including thermal stability [10], mechanical properties [11], flame retardance [12], barrier resistance [13], and anticorrosion properties [14].

These clays such as montmorillonite, kaolin, attapulgite, and mica sericite have all been used to fabricate superabsorbent composites. The incorporation of these mineral powders cannot only reduce production cost, but also can improve the swelling ability, gel strength, mechanical, and thermal stability of the corresponding superabsorbent composites [4].

BENT is a type of clay mainly composed of montmorillonite which is a 2:1 type aluminosilicate. It has a crystalline structure with an octahedral layer of aluminum hydroxide between two tetrahedral layers of silica [15]. The isomorphous substitution of Al^{3+} for Si^{4+} in the tetrahedral layer and Mg^{2+} for Al^{3+} in the octahedral layer results in a net negative surface charge on the BENT. This charge imbalance is offset by exchangeable cations (Na^+ and Ca^{2+}, etc.) at the BENT surface. The layered structure of the clay expands after wetting. Na^+ and Ca^{2+} are strongly hydrated in the presence of water, resulting in a hydrophilic environment at the BENT surface [16].

Conventionally, modified clays with alkyl ammoniums are not suitable for bio-applications due to their toxicity. Chitosan is a good candidate as an intercalant for

BENT modification. Amine groups of chitosan, in acidic solution, are converted to a cationic form ($-NH_3^+$) which is necessary for the cation exchange reaction between the clay and chitosan. Chitosan is extensively used in bio-related applications due to its biocompatibility and biodegradability. Therefore, chitosan-modified clays can be used in the preparation of polymer–clay nanocomposites for bio-applications [1, 5, 9].

In this article, the monomers, Am and 2-acrylamido-2-methyl-1-propane sulfonic acid (AmMPSA) were polymerized in situ with chitosan-intercalated bentonite to give the corresponding nanocomposite hydrogels. The effect of both the ionic monomer and the intercalated bentonite percentages was studied and correlated with the properties of the hydrogels (nanocomposites).

The intercalation was proven by FT-IR analysis, X-ray diffraction, and TEM. The equilibrium swelling capacity, the thermal stability, and the surface morphology were evaluated by various analytic techniques, traditionally applied in studies on nanocomposites, and correlated with the amount of both the ionic monomer AmMPSA and the dispersed intercalated BENT (INT-BENT).

Materials and experimental techniques

Materials

Acrylamide was purchased from S.D. Fine-Chem. Ltd., Boisar, India. AmMPSA, ammonium persulphate (APS), ethylene glycol dimethacrylate (EGDMA) and natural BENT were purchased from Aldrich-Chemical Co., Gillingham-Dorest, England. The Na^+-exchanged form of bentonite used in this study contained about 95% montmorillonite with the chemical composition of 69.32% SiO_2, 14.27% Al_2O_3, 1.99% CaO, 2.69% MgO, 1.84% Fe_2O_3, 1.85% Na_2O, and 1.38% K_2O as reported by the supplier. The cation exchange capacity (CEC) of the clay, measured by the methylene blue method, was 700 mmol/kg.

Chitosan was supplied by Aldrich-Sigma, with an average molecular weight of 342,500 g/mol and a deacetylation degree of $\approx$75%. It is a linear polysaccharide composed of randomly distributed β-(1-4)-linked D-glucosamine (deacetylated unit) and *N*-acetyl-D-glucosamine (acetylated unit).

Experimental techniques

Acid activation of BENT

The specific surface area and the surface acidity of the clay samples can be greatly increased by the acid activation process. Fifteen grams of natural bentonite were activated by refluxing with 200 mL 1:1 (v/v) conc. H_2SO_4 at 60 °C for 2 h in a round-bottom flask. The suspension was cooled in air, filtered off, then washed several times with double-distilled water, and dried in an oven at 120 °C for 2 h prior to use.

Modification of the activated BENT

The activated BENT was modified by chitosan through the cation exchange method. BENT was dispersed in the deionized water at room temperature under continuous mechanical stirring for 24 h followed by the removal of any sediment. The obtained dispersion concentration was 2 wt%. Typically, 2.2526 g chitosan, previously dissolved into 2% acetic acid, was required to interact with the dispersion containing 2 g BENT (based on CEC of BENT and 1:1 interaction). The chitosan solution was slowly added into the BENT dispersion under vigorously stirring for 2 h at 80 °C. The dispersion was cooled down to 60 °C and kept stirring until most of the water was vaporized. After the heat treatment, the mixture was centrifuged, and washed with 2% acetic acid solution and water to get rid of any non-interacted chitosan. The product was dried in an air-circulating oven at 60 °C for 6 h. Then, it was ground and kept in a glass-capped bottle. Also, a domestic microwave oven (Panasonic, model dimension 4, operating frequency of 2.45 GHz, 0.7 kW) and an ultrasound bath (Eyela, Korea) were used for the modification of BENT using microwave irradiation. The time for this irradiation was 180 s. The same treatment was performed for the microwave INT-BENT as mentioned above. The volumes of chitosan solution and BENT dispersion were the same during both treatments in order to make 1:1 chitosan: BENT based on CEC of BENT.

Synthesis of hydrogels

Am/AmMPSA hydrogels were prepared by free radical crosslinking copolymerization of Am monomer, the anionic comonomer (AmMPSA) and the multifunctional crosslinker (EGDMA). To prepare highly swollen Am/AmMPSA hydrogel systems, a predetermined amount of Am was dissolved in 2.0 mL water. Then, the corresponding weight of AmMPSA was added to each Am solution to get the required Am: AmMPSA molar ratio, as shown in Table 1. The solutions were designated as H1-6. To each solution, 0.19 and 0.77 wt% of EGDMA and APS, respectively, based on the total monomers weight, were added. The solutions were placed in cylindrical polypropylene plastic molds (having diameter of 12 mm and height of 100 mm), then, they were polymerized for 24 h in an oven at 50 °C. Transparent gels were obtained after approximately 30 min. The obtained hydrogels were cut into similar disks of 2.5 mm thickness. The disks were thoroughly rinsed with distilled water and dried in air. Am/AmMPSA/INT-BENT composite hydrogels were prepared by using the same preparation method. 2 mL of INT-BENT dispersions of different concentration were added to identical monomer solutions corresponding to H6 as illustrated in Scheme 1.

The obtained composites were designated C*n*, where *n* was denoted to the weight percentage of the thermally INT-BENT based on the monomers weight.

Characterization

FTIR spectroscopy of polymers was recorded in KBr pellets on Nicolet 5700FTIR THERMO.

Table 1 The composition of the as-synthesized hydrogels and composites

Sample code	H1	H2	H3	H4	H5	H6	C3	C6	C9	C12	C15
Am (moles)	9.15	9.005	8.860	8.715	8.570	8.425	8.425	8.425	8.425	8.425	8.425
AmMPSA (moles)	–	0.145	0.290	0.435	0.580	0.725	0.725	0.725	0.725	0.725	0.725
INT-BENT[a] (wt%)	–	–	–	–	–	–	3	6	9	12	15

[a] Intercalation was performed thermally

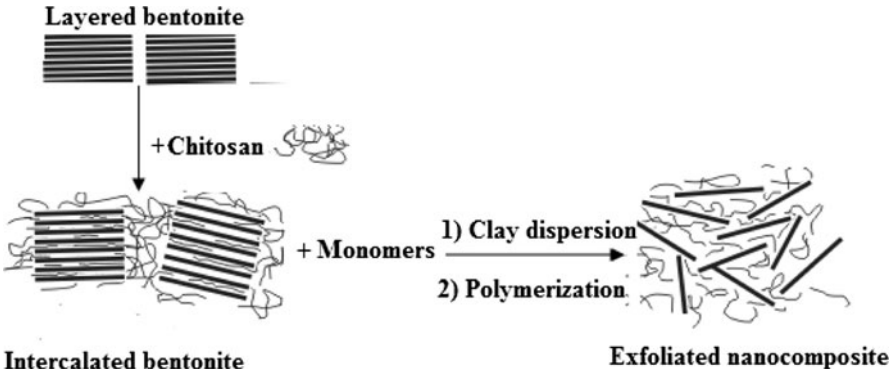

Scheme 1 Bentonite intercalation and the exfoliated nanocomposite formation

X-ray measurement used Co–K radiation, operated at 40 kV and 25 mA. All the samples, for X-ray diffraction measurement, were processed to the powder form.

For morphological characterization, The JEM-2000EX transmission election microscope (TEM) was used at an acceleration voltage of 200 kV. Scanning electron micrographs were taken for both swollen and dry samples. Swollen hydrogels were freeze-dried using a freeze drier (Christ, Germany, Alpha 1-2) at −52 °C for 6 h. Transverse sections were cut from freeze-dried film samples using a cold knife. Samples were then examined with a Jeol JSM-5400 scanning electron microscopy (SEM) (JEOL, Tokyo, Japan).While in the case of the dried specimens; dry samples were coated with a gold metal layer to provide proper surface conduction. Thermograms of the polymeric hydrogels and composites were recorded at a heating rate of 10 °C/min up to 800 °C under N_2 condition using a SDT Q600 (TA Co., USA) thermogravimetric analyzer in the range of 30–800 °C.

Determination of the equilibrium swelling capacity

The swelling study of the hydrogels and the hydrogel composites was carried out, in triplicate, by the gravimetric method. Dry hydrogel disks were immersed in 250 mL distilled water at 25 °C for 24 h to achieve the equilibrium swelling. The samples were weighed, after wiping superficially, by the electronic balance (Sartorius, BP 210S, $d = 0.1$ mg).

The equilibrium swelling capacity Q (g/g) of hydrogels was calculated from the following equation:

$$Q = (M - M_0)/M_0 \quad (1)$$

where M (g) is the weight of the swollen hydrogel after equilibrium swelling and M_0 (g) is the weight of the dry hydrogel Drying was performed at room temperature for about 48 h, until constant weight was obtained.

The results shown below were the average of at least three points measured independently. The weight of any swollen sample was normalized to its dry weight. The standard deviation in all measurements was close to zero. The total uncertainly for all experiments ranged from 3 to 5%.

Results and discussion

FT-IR analysis

In order to obtain an evidence for the intercalation and the composite formation, FT-IR spectra had been recorded in the region of 400–4000 cm^{-1}.

Figure 1a shows the spectrum of pure chitosan with two characteristic bands namely, at 1580 cm^{-1} representing N–H bending and C–N stretching and a strong band between 800 and 1200 cm^{-1} which is characteristic of the presence of the pyranose ring in chitosan. The spectrum of the acid activated-BENT (Fig. 1b) shows that there was a group of absorption peaks between 3447 and 3635 cm^{-1} due to stretching bands of the OH groups. Two characteristic bands, at 1044 and 797 cm^{-1} correspond to Si–O–Si stretching vibrations and Si–O–Al bending vibrations, respectively, appeared. The first band appeared at 1054 cm^{-1}, while the second one appeared at 790 cm^{-1} in the spectrum of the INT-BENT (Fig. 1c). This may confirm the intercalation of chitosan into BENT via an intense specific interaction of BENT with chitosan through hydrogen bonding. This shift in Si–O–Si may be due to the fact that the chitosan adsorbed onto BENT particles improved the facial polarity and the microenvironment of BENT and changed the potential energy. As a result, the inorganic–organic incompatibility was minimized [17].

Interestingly, the bands at 525 and 465 cm^{-1} corresponding to the Al–O (where Al is an octahedral cation) and Mg–O vibrations, respectively, were not shifted after intercalation; this may indicate that both the cations did not participate in the intercalation reaction.

Figure 1d shows the FT-IR spectra of H6. The peak at 1658 cm^{-1} was related to the carbonyl group of the amide groups and that at 1555 cm^{-1} was due to the N–H bending vibration. The much broader absorption peaks in the regions of 3100 and 3500 cm^{-1} were concerned with the N–H bands that interfered with the stretching bands of the OH groups and the NH_2 group. The characteristic absorption peak of AMPS was shown at 1038 cm^{-1} due to SO group. Figure 1e represents the FT-IR spectra of the composite C9. It is worth mentioning that the characteristic peak of SO group coincided with that of Si–O vibrations of the BENT (at 1039 cm^{-1}). The remarkable shift in the characteristic band of the pyranose groups of chitosan after the intercalation and the polymer composite formation may attribute the intercalation interaction and the polymer/clay dispersion to the hydrogen bond formation

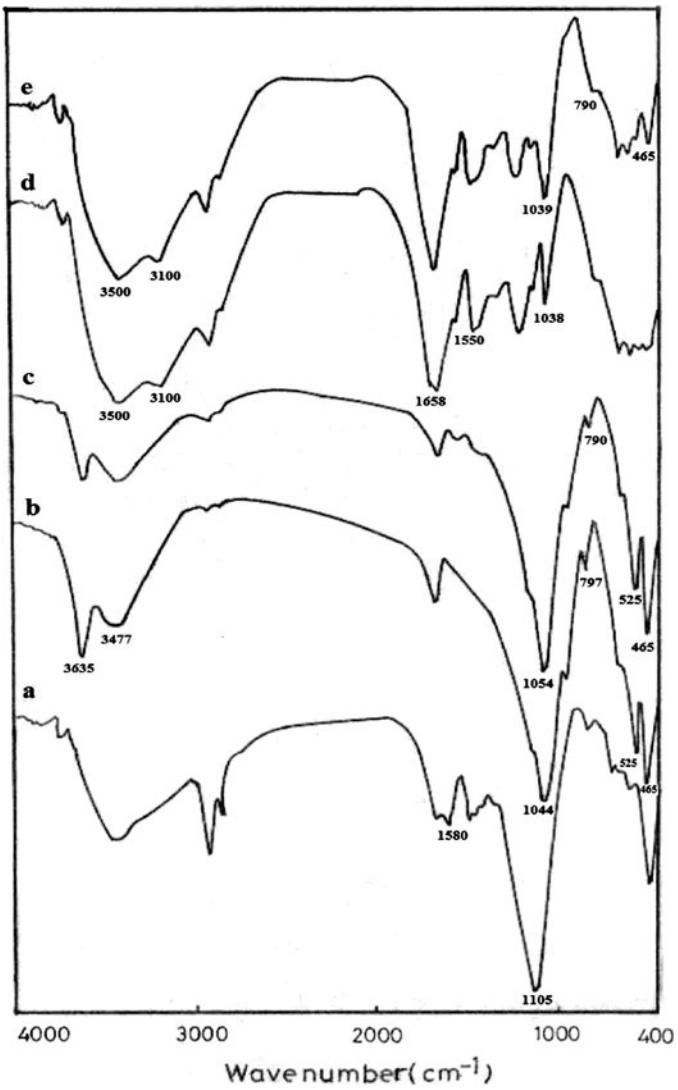

Fig. 1 Infrared spectra. *a* Chitosan, *b* acid-activated bentonite, *c* intercalated bentonite, *d* polymer H6, and *e* composite C9

induced by the presence of these groups. The presence of the characteristic bands of BENT in this spectrum confirms the composite formation.

X-ray diffraction

The change of the clay interlayer distance can be detected by XRD. The XRD pattern in Fig. 2a–d represents the BENT, INT-BENT thermally, INT-BENT by

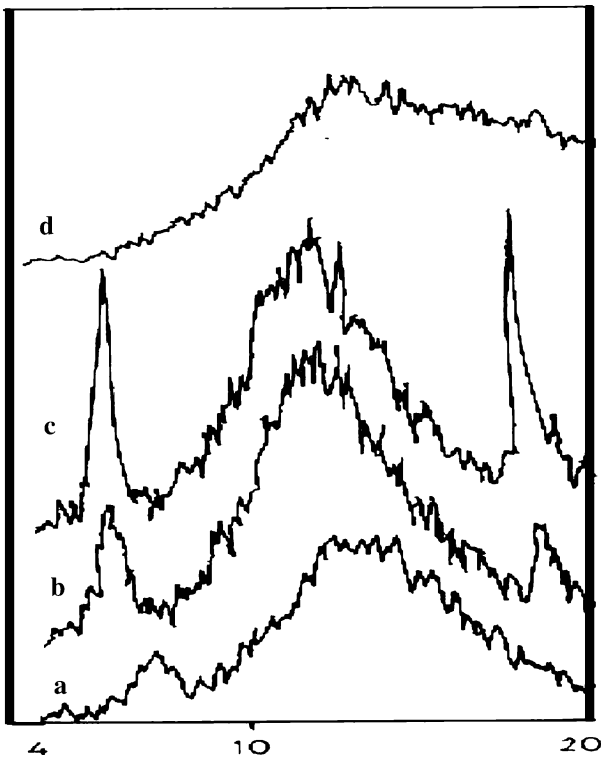

Fig. 2 X-ray diffraction. *a* Bentonite, *b* intercalated bentonite thermally, *c* intercalated bentonite by microwave, and *d* composite C9

microwave irradiation, and the composite C9, respectively. The basal spacing of each sample was calculated using Bragg's law:

$$2d \sin\theta = m\lambda \tag{2}$$

where d is the basal spacing (Å), θ is the angle of diffraction (°), λ is the wavelength (nm), and m is the path differences between the reflected waves which equals an integral number of wavelengths (λ).

Water may be absorbed between the silicate sheets, thus pushing the silicate sheets apart which promotes the diffusion of chitosan into the clay interlayer spaces [18]. The basal spacing for the BENT was 1.21 nm, corresponding to $2\theta = 7.33°$. Intercalation by chitosan increased the basal spacing to 1.31 and 1.4 nm ($2\theta = 6.304°$ and 6.72°, for the microwave irradiated INT-BENT and the thermally INT-BENT, respectively). The microwave irradiation has been assumed to increase the molecular movements of the intercalant between clay layers via different mechanisms but this low increment in the value of the basal spacing probably indicates that the interlayer spaces were not fully expanded by the microwave irradiation. Maybe a considerable amount of the chitosan was adsorbed at the external surface. Thus, the method of intercalation has an important effect on the

interlayer structure of the modified clay mineral. It should be pointed out that the cation exchange reaction between chitosan and the clay is thermodynamically favorable. The Gibbs free energy for adsorption of chitosan on the clay surface is shown in Eq. 3:

$$G = -RT \ln K \tag{3}$$

where R is the gas constant, T is the intercalation temperature, and K is a parameter which depends on the polymer–clay interaction sites. For instance, (G at 323°K is −55.6 kJ/mol, which indicates the high thermodynamic tendency for the adsorption of chitosan on the clay surface. This high negative Gibbs energy indicates that chitosan, in spite of its high thermodynamic volume in comparison with usual low molecular weight cationic intercalants, can diffuse between interlayer distance of the clay. It is valuable to mention that the intercalation reaction is carried out more easily with raising temperature. Diffusion coefficient of intercalant in intercalation media is enhanced with increasing temperature. Therefore, a higher molecular movement of chitosan chains increased the probability for chitosan entrance between clay layers to carry out a successful intercalation reaction [9]. Surprisingly, Chang et al. [19] found that the increase in the operational temperature from 30 to 50 °C is accompanied with a decrease of d-spacing of Na^+-MMT clay due to the evaporation of small molecules existed in the interlayer region. In this investigation, the cation exchange mechanism is the proposed one, although, neutral [10, 19] and anionic [4, 20] polymers had been used as intercalating agents for BENT.

XRD pattern (Fig. 2d) does not show any acute peak; which indicates the existence of exfoliated silicate layers of the precursor BENT dispersed in the polymer background so that the crystalline behavior was suppressed and the clay had been exfoliated in the polymer matrix to form a nanocomposite structure.

Surface morphology

TEM micrograph of INT-BENT Fig. 3a confirms that no aggregates of the clay particles were present and the observed layered morphology may be attributed to the penetration of chitosan chains into BENT silicate layers by means of the intercalation interaction.

The SEM of the dry composite C9, as shown in Fig. 3b reveals that the intercalated particles were finely distributed into the polymer matrix with a good compatibility. The incorporation of BENT and polymer seems to destroy the original structure of BENT and to convert the composite morphology to the amorphous structure. This confirms the exfoliation of the clay particles in the polymer matrix as proven by X-ray patterns as described above.

SEM of freeze-dried water swollen composite C9 was performed; in order to characterize its microstructure as shown in Fig. 3c. It could be observed that the prepared composite is porous, with a three-dimensional interconnected microstructure by virtue of the freeze-drying step with the pores being the result of ice crystal formation. The interconnection between pores could be assigned to the cross-linking network formation in gels. The observable porosity could elucidate the high absorption capacity of such composites.

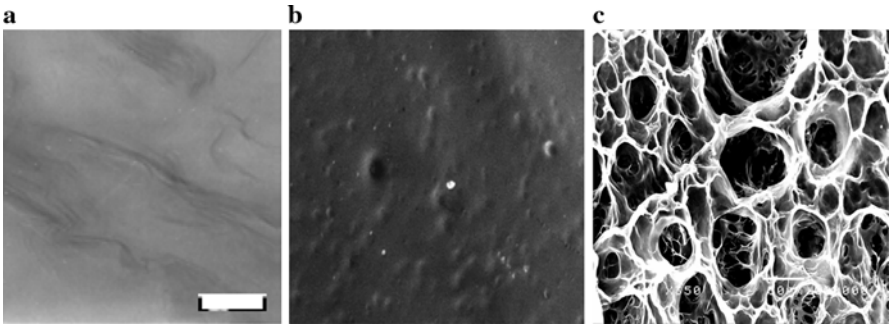

Fig. 3 Surface morphology. *a* TEM micrograph of thermally INT-BENT. The scale bar is 50 nm. *b* scanning electron micrograph for dry C9 composite, and *c* scanning electron micrograph for freeze dried C9 composite hydrogel. The scale bar is 50 μm and the magnification is 350

The swelling capacity

Hydrogels could imbibe water via a combination of many mechanisms, physical entrapment of water via capillary forces in their macro-porous structure, hydration of functional groups and essentially dissolution and thermodynamically favored expansion of the macromolecular chains, which is limited by cross-linkages [6].

When a xerogel is brought into contact with a buffer solution, the solution diffuses into the network and a volume phase transition occurs, resulting in the expansion of the hydrogel. Diffusion involves the migration of the fluid into pre-existing or dynamically formed spaces between the hydrogel chains. Swelling of the hydrogel involves large segmental motion resulting, ultimately, in the increased separation of the hydrogel chains. The swelling behavior was followed by the degree of swelling, until thermodynamic equilibrium was reached. The swelling equilibrium occurs when the values of the osmotic force driving the solvent into the network and of the elastic force of the stretched sub-chains become equal [21].

AmMPSA received a great attention in recent years due to its strongly ionizable sulfonate group. The synthesis of Am/AmMPSA via radical chain polymerization is a well-established procedure. AmMPSA dissociates completely in the overall pH range, and therefore, the hydrogels derived from AmMPSA exhibit a pH independent swelling behavior.

The capacity of swelling is one of the most important parameters to evaluate the property of hydrogels.

Table 2 illustrates the equilibrium swelling capacity of the as-synthesized Am/AmMPSA hydrogels with different ionic monomer content. As shown in this table,

Table 2 The equilibrium swelling capacity of the as-synthesized hydrogels and composite hydrogels

Sample code	H1	H2	H3	H4	H5	H6	C3	C6	C9	C12	C15
Q (g/g)	17	23	36	46	87	94	127	134	140	169	180

the equilibrium swelling capacity increased with the increase in the ionic content which may be attributed to the increased repulsion between sulfonate groups that could lead to an extra hydrogel network expansion [4, 5].

Table 2 also illuminates the role of the INT-BENT content dispersed in the H6. Clearly, the INT-BENT could promote the equilibrium swelling capacity within the range of the investigated concentration. This may be explained by the hydrophilicity of BENT and/or the presence of chitosan chains throughout the layers of BENT. This is in contrary with a recent work [22] observing that any amount of the cationic intercalant [poly(dimethyldiallylammonium chloride)] would not encourage the swelling capacity of the starch-g-acrylic acid/Na-bentonite hydrogel composite due to the increased salt bonding between the carboxylate groups and the quaternary ammonium groups.

In the literature data, the experimental observations have not been unified with respect to the effect of clay moiety, dispersed in a polymeric matrix, on the swelling capacity; many authors [4, 23] concluded that the hydrophilic clay could have the positive effect on the swelling while other authors observed a negative one [20, 24]. We believe that the particle size, chemistry (origin and surface treatment), and content of the clay are the determinant factors that establish the outcome of the clay, incorporated in a composite, on its swelling.

For example, but not limited, quaternary ammonium salts were also often used to modify clay surface to change the interaction between clay and polymeric network, and then improve swelling behaviors of resulting superabsorbent composites [25, 26]. Main components of clay may also influence properties of corresponding superabsorbent composite; however, no information about this has been reported until now. In fact, the cations on the surface and in channels of clay may enhance osmotic pressure difference between polymeric network and external solution, and then increase equilibrium water absorbency. Furthermore, the cations could form intramolecular and intermolecular complex with hydrophilic groups on the polymer chains, and then improve hydrogel strength of corresponding superabsorbent composites [27, 28].

Thermal stability of the as-synthesized composites

The formation of nanocomposites is usually related to the change in thermal properties of the polymer [10]. The thermal stability is the ability of a material to maintain its physical properties when exposed to high temperatures and is generally estimated from the weight loss upon heating which results in the formation of volatile products [8].

The thermogram Fig. 4a of the prepared hydrogel "H6" reveals two main weight-loss stages. Desorption of the physically adsorbed water occurred at 100 °C while that absorbed by the polymer by different binding modes might evaporate during the first stage. The polymer thermal degradation was initiated by scissions of head-to-head linkages (H–H) at 140–160 °C as a first step, depending on the heating rate. The second step (200–300 °C) was initiated by scission at the vinylidene chain-end units and the third step (above 300 °C) was initiated by random scissions

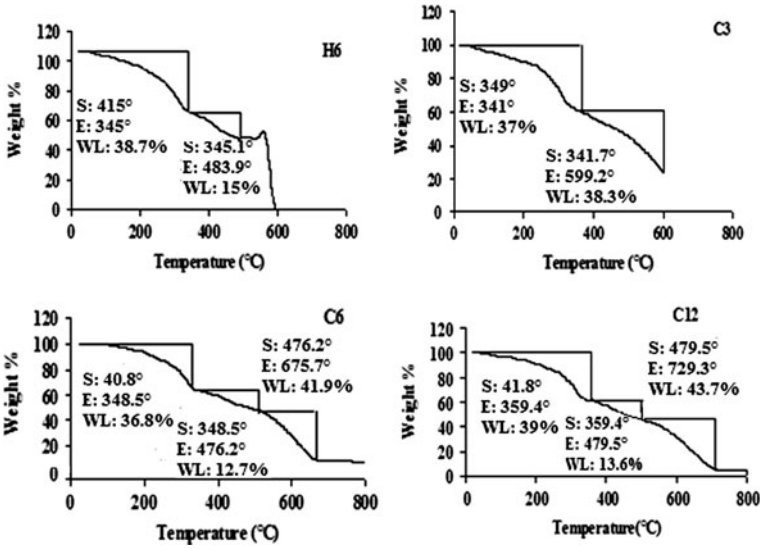

Fig. 4 TGA. *a* Polymer H6, *b* composite C3, *c* composite C6, and **d** composite C12

within the polymer chain [10], accordingly, the onset of the polymer backbone cleavage or so-called carbonation was probably in the second stage.

Figure 4b–d represent the thermograms of the prepared composites. Composite C3 showed two main regions of degradation while C6 and C12 showed three regions. The gradual increase in the degradation temperature as the content of INT-BENT increased from C3 to C12 confirms the enhanced thermal stability of theses composites.

Although chitosan has a rigid backbone with strong inter- or intra-molecular hydrogen bonding [29], its initial degradation might occur before 300 °C.

It is worth mentioning that water absorbed by chitosan intercalated in the interlayer space of BENT might evaporate at a higher temperature than that absorbed by the free polymer since water associated with the free polymer should have the lowest binding energy. The dehydroxylation of the aluminosilicate layer of BENT occurred beyond 500 °C.

It may be concluded that the prepared composites were more thermally stable materials than the polymeric hydrogel. This may be additional evidence that the bentonite layers were exfoliated and dispersed in the polymer matrix. The improvement of thermal stability can be attributed to the barrier effect of BENT [8, 23]; BENT is a layered structure and small molecules generated during thermal decomposition process cannot permeate, i.e. hindered to diffuse, and thus have to bypass BENT layers. The improved thermal stability is a common advantage induced by inorganic fillers [30]. It is noteworthy to mention that the intercalation by polymers is usually preferred than that by cationic surfactants due to a decrease in thermal stability of the organoclays inclined by a surfactant. Besides, it makes no contribution to the mechanical strength [31].

Conclusion

A series of hydrogels and composites was synthesized by the solution polymerization technique. These hydrogels were composed of Am and AmMPSA as an ionic monomer. Intercalation of BENT using chitosan was performed in order to disperse the intercalated particles into the polymer matrix; aiming at preparing superabsorbent composite hydrogels. The following conclusions are drawn from the present investigation:

FT-IR showed that the remarkable shift in the characteristic band of the pyranose group of chitosan after the intercalation and the polymer composite formation may attribute the intercalation interaction and the polymer/clay dispersion to the hydrogen bond formation induced by the presence of pyranose groups of chitosan.

XRD showed that intercalation by chitosan increases the basal spacing of BENT and the method of the intercalation affects the value of the basal spacing. Also, the clay crystalline behavior was suppressed as it had been exfoliated in the polymer matrix to form a nanocomposite structure.

In addition, a noticeable enhancement in water equilibrium swelling capacity was a result of any increment in the ionized monomer or INT-BENT content.

The exfoliated BENT layers did improve the thermal stability of the prepared composites.

Intercalation was a simple, but an effective way to modify BENT and improve its compatibility with the polymer since the dispersion of clay platelets directly affects the final structure and thus the final properties of the polymer nanocomposites.

Thus, this bio-modified nanoclay as well as its possible polymer nanocomposites can be used in a variety of applications especially biomedicine. Furthermore, since the primary component is water, these nanocomposite superabsorbent hydrogels can be utilized as environmentally friendly rubbery materials in the management of resources and waste, and may open new doors in various areas of advanced research and technology.

References

1. Pourjavadi A, Mahdavinia GR (2006) Superabsorbency, pH-sensitivity and swelling kinetics of partially hydrolyzed chitosan-g-poly(acrylamide) hydrogels. Turk J Chem 30:595–608
2. Kabiri K, Zohuriaan-Mehr J (2004) Superabsorbent hydrogels from concentrated solution terpolymerization. Iran Polym J 13:423–430
3. Zhao Y, Su H, Fang L, Tan T (2005) Superabsorbent hydrogels from poly(aspartic acid) with salt-, temperature- and pH-responsiveness properties. Polymer 46:5368–5376
4. Kundakci S, Üzüm ÖB, Karadağ E (2008) Swelling and dye sorption studies of acrylamide/2-acrylamido-2-methyl-1-propanesulfonic acid/bentonite highly swollen composite hydrogels. React Funct Polym 68:458–473
5. Liu J, Wang Q, Wang A (2007) Synthesis and characterization of chitosan-g-poly(acrylic acid)/sodium humate superabsorbent. Carbohydr Polym 70:166–173
6. Zohuriaan-Mehr MJ, Kabiri K (2008) Superabsorbent polymer materials: a review. Iran Polym J 17:451–477
7. Gao D, Heimann RB (1993) Structure and mechanical properties of superabsorbent poly(acrylamide)-montmorillonite composite hydrogels. Polym Gels Netw 1:225–246

8. Zeng QH, Yu AB, Lu GQ, Paul DR (2005) Clay-based polymer nanocomposites: research and commercial development. J Nanosci Nanotechnol 5:1574–1592
9. Kabiri K, Mirzadeh H, Zohuriaan-Mehr MJ (2007) Highly rapid preparation of a bio-modified nanoclay with chitosan. Iran Polym J 16:147–151
10. Huskic M, Žigon M (2007) PMMA/MMT nanocomposites prepared by one-step in situ intercalative solution polymerization. Eur Polym J 43:4891–4897
11. Shi X, Xu S, Lin J, Feng S, Wang J (2009) Synthesis of SiO_2-polyacrylic acid hybrid hydrogel with high mechanical properties and salt tolerance using sodium silicate precursor through sol–gel process. Mater Lett 63:527–529
12. Sahoo PK, Samal R (2007) Fire retardancy and biodegradability of poly (methyl methacrylate) nanocomposite. Polym Degrad Stabil 92:1700–1707
13. Yeh JM, Chang KC (2008) Polymer/layered silicate nanocomposite anticorrosive coatings. J Ind Eng Chem 14:275–291
14. Olad A, Rashidzadeh A (2008) Preparation and anticorrosive properties of PANI/Na-MMT and PANI/O-MMT nanocomposites. Prog Org Coat 62:293–298
15. Li Q, Yue QY, Su Y, Gao BY, Fu L (2007) Cationic polyelectrolyte/bentonite prepared by ultrasonic technique and its use as adsorbent for reactive blue K-GL dye. J Hazard Mater 147:370–380
16. Özcan S, Özcan A (2004) Adsorption of acid dyes from aqueous solutions onto acid-activated bentonite. J Colloid Interface Sci 276:39–46
17. Zheng L, Xu S, Peng Y, Wang J, Peng G (2007) Preparation and swelling behavior of amphoteric superabsorbent composite with semi-IPN composed of poly(acrylic acid)/Ca-bentonite/poly(dimethyldiallylammonium chloride). Polym Adv Technol 18:194–199
18. Lovoll G, Sandnes B, Meheust Y, Maloy KJ, Fossum JO, Da Silva GJ, Mundim MSP, Droppa R Jr, Fonseca DM (2005) Dynamics of water intercalation fronts in a nanolayered synthetic silicate: a synchrotron X-ray scattering study. Phys B Condens Matter 370:90–98
19. Chang KC, Chen ST, Lin HF, Lin CY, Huang HH, Yeh JM, Yu YH (2008) Effect of clay on the corrosion protection efficiency of PMMA/Na^+-MMT clay nanocomposite coatings evaluated by electrochemical measurements. Europ Polym J 44:13–23
20. Zhang J, Yuan K, Wang YP, Gu SJ, Zhang ST (2007) Preparation and properties of polyacrylate/bentonite superabsorbent hybrid via intercalated polymerization. Mater Lett 61:316–320
21. Tomić SL, Mićic′ MM, Filipović JM, Suljovrujić EH (2007) Swelling and drug release behavior of poly (2-hydroxyethyl methacrylate/itaconic acid) copolymeric hydrogels obtained by gamma irradiation. Rad Phys Chem 76:801–810
22. Huang X, Xu S, Zhong M, Wang J, Feng S, Shi R (2009) Modification of Na-bentonite by polycations for fabrication of amphoteric semi-IPN nanocomposite hydrogels. Appl clay Sci 42:455–459
23. Santiago F, Mucientes AE, Osorio M, Rivera C (2007) Preparation of composites and nanocomposites based on bentonite and poly(sodium acrylate). Effect of amount of bentonite on the swelling behavior. Europ Polym J 43:1–9
24. Xu K, Wang J, Xiang S, Chen Q, Yue Y, Su X, Song C, Wang P (2007) Polyampholytes superabsorbent nanocomposites with excellent gel strength. Compos Sci Technol 67:3480–3486
25. Alexandre M, Beyer G, Henrist C, Cloots R, Rylmont A, Jerome R, Dubois P (2001) One-pot preparation of polymer/clay nanocomposties starting from Na^+ montmorillonite. 1. Melt intercalation of ethylene-vinyl acetate copolymer. Chem. Mater 13:3830–3832
26. Zhang W, Liang Y, Luo W, Fang Y (2003) Effects of clay-modifying agents on the morphology and properties of poly(methyl methacrylate)/clay nanocomposites synthesized via γ-ray irradiation polymerization. J Polym Sci A 41:3218–3226
27. Lee W, Su C (1998) Superabsorbent polymeric materials. V.Synthesis and swelling behavior of sodium acrylate and sodium 2-acrylamido-2-methyl-1-propanesulphonate copolymeric gels. Appl Polym Sci 69:229–237
28. Zhang J, Zhao Y, Wang A (2007) Superabsorbent composite. XIII. Effects of [Al.sup. 3+]-attapulgite on hydrogel strength and swelling behaviors of poly (acrylic acid)/[Al.sup.3+]-attapulgite superabsorbent composites. Polym Eng Sci 47:619–624
29. Kaewpirom S, Boonsang S (2006) Electrical response characterisation of poly(ethylene glycol) macromer (PEGM)/chitosan hydrogels in NaCl solution. Eur Polym J 42:1609–1616
30. Günister E, Pestreli D, Ünlü CH, Atici O, Güngör N (2007) Synthesis and characterization of chitosan-MMT biocomposite systems. Carbohyd Polym 67:358–365
31. Xu S, Zhang S, Yang J (2008) An amphoteric semi-IPN nanocomposite hydrogels based on intercalation of cationic polyacrylamide into bentonite. Mater Lett 62:3999–4002